Korean J. Chem. Eng., **29**(11), 1628-1637 (2012)
DOI: 10.1007/s11814-012-0070-8

Modeling of P-ρ-T properties of ionic liquids using ISM equation of state: Application to pure component and binary mixtures

Mohammad Mehdi Papari*, Sayed Mostafa Hosseini,†, Fatemeh Fadaei-Nobandegani**, and Jalil Moghadasi****

*Department of Chemistry, Shiraz University of Technology, Shiraz 71555-313, Iran
**Department of Chemistry, Shiraz University, Shiraz 71454, Iran
(*Received 28 February 2012 • accepted 19 May 2012*)

Abstract−Ihm-Song-Mason (ISM) equation of state (EOS) has been previously employed for modeling the volumetric properties of ionic liquids (ILs). The novelty of the present work is in replacing the macroscopic scaling constants with microscopic ones. Three temperature-dependent parameters that appeared in the EOS, which are universal functions of the reduced temperature, were determined using these new microscopic scaling constants. These parameters are the effective hard-sphere diameter (σ) and the non-bonded interaction energy between two spheres (ε). The present EOS is evaluated by examination of 3997 experimental density data points for five classes of ILs. The average absolute deviation (AAD) of the calculated densities from literature values was found to be of the order of 0.38%. Our calculations involved a broad range of temperature from 293 K to 472 K and pressures from 0.1 MPa up to 200 MPa. Another aspect of the present study is the extension of the proposed EOS to predict density of binary mixtures involving IL+ water and IL+ IL. In the case of binary mixtures, 898 data points were taken to assess the capability of the EOS. The overall AAD of the calculated mixture densities from the literature ones was within 0.43%.

Key words: Equation of State, Ionic Liquid, Binary Mixture

INTRODUCTION

Ionic liquids (ILs) have come into focus recently as new materials offering several highly promising applications. The unique properties of these liquids, such as non-flammability, electric conductivity, thermal stability, low vapor pressure and high heat capacity lead to this fact that they are more considered than conventional organic solvents. Their potential applications can be briefly cited: 1) they are favorite electrolytes in lithium rechargeable batteries [1] and super-capacitors [2]; 2) These materials can also be used as thermal fluids for heat storage by combining of their high heat capacity, thermal stability and negligible vapor pressure [3]; and 3) Their interesting solvent properties make them well-known as green solvents for the future [4].

The relationship between pressure, volume and temperature is one of the most fundamental and useful from both a theoretical and practical point of view. PVT data are particularly important to describe the thermodynamic behavior of ILs and are important for efficient design of chemical products and processes. The two most commonly used methods of calculating PVT properties are equation-of-state (EOS) and PVT correlations.

Recently, several models have been proposed for predicting densities of this class of fluids. Wang et al. [5] used a group contribution equation of state, which was based on electrolyte perturbation theory to calculate densities of ionic liquids. They divided ILs into several groups including cations, anions, and alkyl substituent groups. Shen et al. [6] predicted the densities of ILs using the Patel-Teja equation of state in conjunction with the modified Lydersen-Joback-Reid group contribution method. Machida et al. [7] modified the temperature dependence of Sanchez-Lacombe EOS to take into account the hydrogen bonding and ionic interactions appearing in ILs. Further Abildskov et al. [8,9] described a method for correlating the liquid densities of ILs based on a corresponding states form for the direct correlation function integrals. They extended their method to model the phase behavior of mixtures of ionic liquids and organic solvents [10]. It should be mentioned that some computational methods have also been proposed for predicting densities of ionic liquids. For example, Palomar et al. [11] used COSMO-RS predictive model which was based on the quantum chemistry. Trohalaki et al. [12] reported a QSPR method for the density calculations. Valderama et al. [13] presented an artificial neural networks and group contribution method to correlate the density of ILs. Aparicio et al. [14] reviewed the available predictive models as well as experimental data reported in literature for the thermophysical properties and especially density and PVT behavior of ionic liquids. Kim et al. [15] also presented an EOS method based on the group contribution non-random lattice-uid (NLF) model for predicting the density and solubility of carbon dioxide in ILs. Their results showed that the GC-EOS is applicable for methylimidazolium-based IL systems in predicting properties and solvent design.

The present work is a continuation of our studies on predicting volumetric properties of ILs using Ihm-Song-Mason (ISM) equation of state [16]. Recent work by Hosseini and Sharafi [17] led to extension of ISM EOS to predict the pressure-volume-temperature (PVT) properties of pure ILs. The novelty of the present work is replacing the macroscopic scaling constants such as surface [17,18] and critical properties [19-21] in the three temperature-dependent parameters appearing in the ISM EOS by the effective hard-sphere diameter (σ) and the non-bonded interaction energy (ε). This replace-

†To whom correspondence should be addressed.
E-mail: seied_mostafa_hosseini@yahoo.com

Table 1. The entire ILs studied in this work

Ionic liquid	IUPAC name
$[C_4mim][NTf_2]$	1-Butyl-3-methylimidazolium bis[(trifluoromethyl)sulfonyl]imide
$[C_5mim][NTf_2]$	1-Pentyl-3-methylimidazolium bis[(trifluoromethyl)sulfonyl]imide
$[C_2mim][NTf_2]$	1-Ethyl-3-methylimidazolium bis[(trifluoromethyl)sulfonyl]imide
$[C_4mim][Triflate]$	1-Butyl-3-methylimidazolium trifluoromethanesulfonate
$[C_2mim][BF_4]$	1-Ethyl-3-methylimidazolium tetrafluoroborate
$[C_4mim][BF_4]$	1-Butyl-3-methylimidazolium tetrafluoroborate
$[C_6mim][BF_4]$	1-Hexyl-3-methylimidazolium tetrafluoroborate
$[C_8mim][BF_4]$	1-Ocyl-3-methylimidazolium tetrafluoroborate
$[(C_6H_{13})_3P(C_{14}H_{29})][Cl]$	Trihexyltetradecylphosphonium chloride
$[(C_6H_{13})_3P(C_{14}H_{29})][Ac]$	Tetradecyl (trihexyl)phosphonium acetate
$[(C_6H_{13})_3P(C_{14}H_{29})][NTf_2]$	Trihexyltetradecylphosphonium bis[(trifluoromethyl)sulfonyl]imide
$[(C_6H_{13})_3P(C_{14}H_{29})][N(CN)_2]$	Trihexyltetradecylphosphonium dicyanimide
$[C_2mim][Triflate]$	1-Ethyl-3-methylimidazolium trifluoromethanesulfonate
$[C_6mim][NTf_2]$	1-Hexyl-3-methylimidazolium bis[(trifluoromethyl)sulfonyl]imide
$[C_7mim][NTf_2]$	1-Heptyl-3-methylimidazolium bis[(trifluoromethyl)sulfonyl]imide
$[C_{10}mim][NTf_2]$	1-Decyl-3-methylimidazolium bis[(trifluoromethyl)sulfonyl]imide
$[C_8mim][NTf_2]$	1-Octyl-3-methylimidazolium bis[(trifluoromethyl)sulfonyl]imide
$[C_3mpy][NTf_2]$	3-Methyl-1-propylpyridinium bis[(trifluoromethyl)sulfonyl]imide
$[C_3mpyr][NTf_2]$	3-Methyl-1-propylpyrrolidinium bis[(trifluoromethyl)sulfonyl]imide
$[C_4mpyr][NTf_2]$	1-Butyl-1-methylpyrrolidinium bis[(trifluoromethyl)sulfonyl]imide
$[C_4mim][C(CN)_3]$	1-Butyl-3-methylimidazolium tricyanomethane
$[C_3mim][NTf_2]$	1-Propyl-3-methylimidazolium bis[(trifluoromethyl)sulfonyl]imide
$[N_{1114}][NTf_2]$	Butyltrimethylammonium bis(trifluoromethylsulfonyl)imide
$[C_4mim][PF_6]$	1-Butyl-3-methylimidazolium hexafluorophosphate
$[C_6mim][PF_6]$	1-Hexyl-3-methylimidazolium hexafluorophosphate
$[C_8mim][PF_6]$	1-Octyl-3-methylimidazolium hexafluorophosphate
$[C_4mim][OcSO_4]$	1-Butyl-3-methylimidazolium octylsulphate
$[C_2mim][OcSO_4]$	1-Ethyl-3-methylimidazolium octylsulphate
$[C_2mim][EtSO_4]$	1-Ethyl-3-methylimidazolium ethylsulphate
$[C_3mpip][NTf_2]$	3-Methyl-1-methyl pyrrolidinium bis[(trifluoromethyl)sulfonyl]imide

ment will help improve the accuracy of the proposed EOS. The lack of surface and critical properties of ILs in literature has encouraged us to search for an alternative method to construct ISM EOS. Although surface properties may be easier to measure than the critical ones [22,23], the surface tension is not a property that can be measured with high accuracy. The present EOS is evaluated by examination of 3997 experimental density data points for five classes of ILs. The average absolute deviation (AAD) of the calculated densities from literature values was found to be of the order of 0.38%. Our calculations encompass the temperatures from 293 K to 472 K and the pressures from 0.1 MPa up to 200 MPa. Furthermore, the outcome of the computations is compared with the methods proposed by Gardas-Coutinho (G & C) [24] and Jacquemin et al. (JAC) [25,26]. G & C have extended the Ye and Shreeve [27] group contribution model to estimate the density as a function of the temperature and pressure of a variety of ionic liquids. Furthermore, the density and the excess volumetric properties of fluid mixtures, which depend on the composition and/or temperature, and are of great importance in understanding the nature of molecular aggregation that exists in the binary mixtures, have been determined. In this respect, the extension of the present EOS to binary mixtures IL+water and that IL+IL will also be discussed. 898 data points of binary mixtures were taken to evaluate the capability of the EOS in predicting the mixture densities. The overall AAD of the calculated mixture densities from the literature ones was within 0.43%. Table 1 lists the abbreviations and IUPAC name of studied ILs.

THEORY

1. Equation of State for Pure ILs

The general frame of the ISM EOS is [16]:

$$\frac{P}{\rho kT}=1+\frac{(B_2(T)-\alpha(T))\rho}{1+0.22\lambda b(T)\rho}+\frac{\alpha(T)\rho}{1-\lambda b(T)\rho} \quad (1)$$

Where P is the pressure, ρ is the molar (number) density, $B_2(T)$ is the second virial coefficient, $\alpha(T)$ is the contribution of repulsive branch of pair potential function in the second virial coefficient. This is based on the recognition that the structure of a liquid is determined primarily by repulsive forces, so that fluids of hard bodies can serve as useful reference states. b(T) reflects the van der Waals covolume, kT is the thermal energy per one molecule. λ is a free parameter which can be fixed with the help of volumetric proper-

ties of dense fluids. Any uncertainty in the parameters B_2, α(T), and b(T) can be compensated for by selecting a proper values of λ parameter.

2. Parameter Estimation

The ISM equation of state requires the usage of the second virial coefficient, B_2(T), along with the parameters α(T) and b(T). For central force fields, the second virial coefficient is related to the intermolecular potential energy u(r) through the following equation:

$$B_2(T) = 2\pi N_A \int_0^{\infty} (1 - e^{-u(r)/kT}) r^2 dr \quad (2)$$

Where N_A is Avogadro's number.

If a two-parameter potential energy function u(r) can describe the nature of the interaction potential between particles of a fluid, the potential can be written in dimensionless form by:

$$\frac{u}{\varepsilon} = F\left(\frac{r}{\sigma}\right) \quad (3)$$

where ε is a characteristic energy parameter and σ is a characteristic size parameter, and F is a universal function of the reduced intermolecular separation. Upon substitution, Eq. (2) can be rewritten in dimensionless form:

$$\frac{B_2(T)}{2\pi N_A \sigma^3} = \int_0^{\infty} \left[1 - \exp\left(\frac{-\varepsilon F(r/\sigma)}{k_B T}\right)\right] \left(\frac{r}{\sigma}\right)^2 d\left(\frac{r}{\sigma}\right) \quad (4)$$

It follows from the above equations that the second virial coefficients can be correlated by data reduction with energy and distance parameters as characteristic parameters. This equation also says that the reduced second virial coefficient is a generalized function of the reduced temperature. This function can be determined either by a direct correlation of experimental data for the second virial coefficient or by specification of the universal potential function u/ε and integration. In this work, we have taken ε as the energy parameters and σ as the size parameter in the potential energy relation.

It was empirically found that σ^3 is proportional to the reciprocal density at 298 K and ε/k is proportional to $\Delta H^{vap}/R$. Figs. 1 and 2 illustrate the correlation of heat of vaporization with ε and density at room temperature with σ, respectively. It should be mentioned that if the intermolecular potential is not available, knowledge of experimental second virial coefficient data is sufficient to calculate values of the other two temperature-dependent parameters [16].

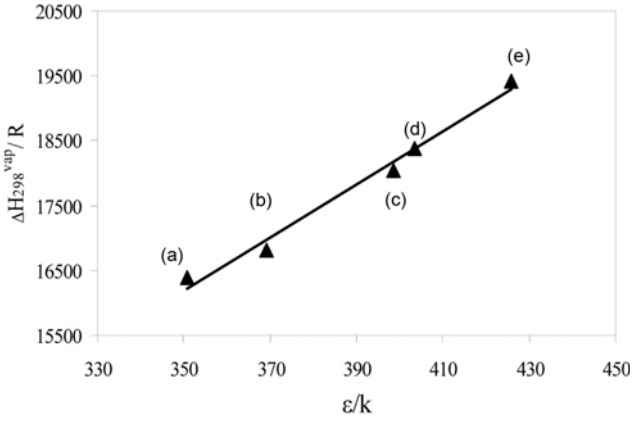

Fig. 1. The linear correlation of ε/k values with ΔH^{vap}_{298}/R for some examples of studied ILs. The filled triangles represent our calculations in this work, and (—) indicates the straight line passing through the points. [C_4mim][NTf_2] (a), [C_6mim][NTf_2] (b), [C_8mim][NTf_2] (c), [C_{10}mim][NTf_2] (d) and [C_4mim][$C(CN)_3$] (e).

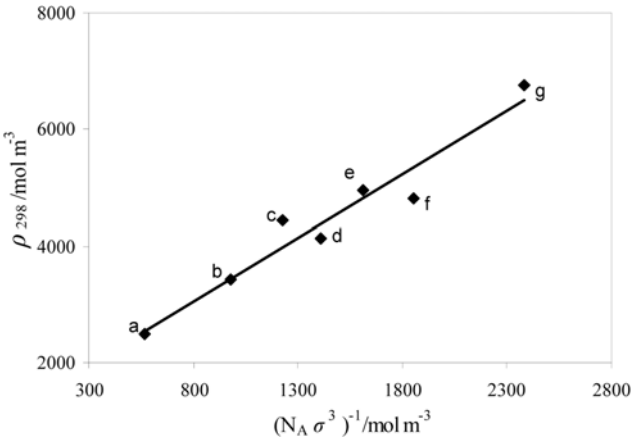

Fig. 2. The linear correlation of $1/(N_A \sigma^3)$ values with room-temperature density for some examples of studied ILs. The filled markers represent our calculations in this work, and (—) indicates the best line passing through the points. [C_{10}mim][NTf_2] (a), [C_4mim][NTf_2] (b), [C_4mim][$C(CN)_3$] (c), [C_6mim][PF_6] (d) [C_2mim][$EtSO_4$] (e), [C_4mim][PF_6] (f) and [C_2mim][BF_4] (g).

The resulting correlation equation for B_2 can be represented by the empirical expression:

$$B_2(T)/(N_A\sigma^3) = 1.033 - 3.0069T_r^{-1} - 10.588T_r^{-2} + 13.096T_r^{-3} - 9.8968T_r^{-4} \quad (5)$$

with:

$$T_r = (kT/\varepsilon) \quad (6)$$

Other temperature dependent parameters can also be correlated with reduced temperature with the following equations:

$$\alpha(T)/(N_A\sigma^3) = a_1[epx(-c_1T_r)] + a_2[1 - \exp(-c_2/T_r^{1/4})] \quad (7)$$

and

$$b(T)/(N_A\sigma^3) = a_1[(1 - c_1T_r)\exp(-c_1T_r)] + a_2[1 - (1 + 0.25c_2/T_r^{1/4})\exp(-c_2/T_r^{1/4})] \quad (8)$$

a_1=−0.0860 c_1=0.5624

a_2=2.3988 c_2=1.4267

The coefficients a_1-c_2 have been determined from the experimental PρT data at high density region.

Briefly, the corresponding-states correlations have been based on several factors: a) the critical constants [28], b) the heat of vaporization and the liquid density at the freezing point [29], c) the surface tension and the liquid density at the freezing point [30,31], d) the boiling points [32], and e) the speed of sound [33,34].

3. Extension to Binary Mixtures

The mixture version of the ISM EOS is as follows [35]:

$$\frac{P}{\rho kT} = 1 + \rho \sum_i \sum_j x_i x_j (B_{ij} - \alpha_{ij}) F_{ij} + \rho \sum_i \sum_j x_i x_j G_{ij} \alpha_{ij} \quad (9)$$

where α is a correction factor for the softness of the repulsive forces and G is the average pair distribution function at contact for additive non-spherical hard-convex bodies. The summations run over all the components of mixtures and subscripts ij refer to the i-j interactions. The parameters F_{ij} and G_{ij} are defined as:

$$F_{ij}=\frac{1}{1-\xi_3}-\left(\frac{b_i b_j}{b_{ij}}\right)^{1/3}\frac{\rho\sum_k x_k b_k^{2/3}(0.22\lambda_k+0.25)}{(1-\xi_3)\left(1+0.22\rho\sum_k x_k b_k\lambda_k\right)} \tag{10}$$

$$G_{ij}=\frac{1}{1-\xi_3}-\left(\frac{b_i b_j}{b_{ij}}\right)^{1/3}\frac{\rho\sum_k x_k b_k^{2/3}(\lambda_k+0.25)}{(1-\xi_3)\left(1+\rho\sum_k x_k b_k\lambda_k\right)} \tag{11}$$

with

$$\xi_3=\frac{\rho}{4}\sum_k x_k b(T)_k \tag{12}$$

The present method for calculating the second virial coefficient and the other two temperature-dependent parameters can be extended to mixtures by using a simple geometric mean for the non-bonded interaction energy parameter, ε and a arithmetic mean for the effective hard-sphere diameter:

$$(\varepsilon/k)_{ij}=\sqrt{(\varepsilon/k)_i(\varepsilon/k)_j} \tag{13}$$

$$\sigma_{ij}=\frac{1}{2}(\sigma_i+\sigma_j) \tag{14}$$

The excess molar volume, V^E of binary mixtures was calculated by taking the effects of additive hard-spheres into account from the following equation and Eqs. (9)-(12):

$$V^E=\frac{x_1M_1+x_2M_2}{\rho_{mix.}}-\frac{x_1M_1}{\rho_1}-\frac{x_2M_2}{\rho_2} \tag{15}$$

Where $\rho_{mix.}$ is the density of mixture involving, x_1 and x_2 are mole fractions and M_1 and M_2 are molar masses associated with two components (1) and (2), respectively.

RESULTS AND DISCUSSION

An EOS for ionic liquids was developed based on statistical-mechanical theory. A microscopic correlation was constructed for the second virial coefficients of ILs using ε and σ as scaling parameters.

To apply this EOS to ILs, the values of parameters λ, ε and σ appearing in Eq. (1) and Eqs. (5)-(8) must be known. In this regard, the heat of vaporization and density at room temperature (ρ_{298}) for several ILs were correlated with ε and σ, respectively. Figs. 1 and 2 illustrate the correlation of heat of vaporization with ε and density at room temperature [36] with σ, correspondingly.

The values of λ appearing in Eq. (1) were found empirically from the PVT data of dense pure components. These parameters for all studied ILs are listed in Table 2. This method for determining λ makes the whole procedure self-correcting, because if the input values of ε and σ are not accurate, the effect will be largely compensated in the determination of λ.

By applying the corresponding states correlations for B_2, α and b as well as λ parameter to the ISM EOS, the density of 30 pure ILs involving imidazolium, phosphonium, pyridinium, pyrrolidinium and ammonium cations over a wide range of temperatures from 293 K to 472 K and pressures from 0.1 MPa up to 200 MPa were predicted. To provide extensive testing and evaluation, we performed a comprehensive comparison with experimental data over a vast range of temperatures and pressures; the calculated densities were compared with those reported in literature [25,37-52]. Our computation results are summarized in Table 3. As the Table 3 shows, the average absolute deviation percent (AAD %) of the calculated density for 3997 literature data points from the experimental values was found to be 0.38%.

Table 2. The input constants for the ISM EOS

Ionic liquid	M_w (gr/mol)	ε/k (K)	σ (nm)	λ
$[C_4mim][OcSO_4]$	348.50	407.43	1.2295	0.15743
$[C_2mim][OcSO_4]$	320.45	406.80	1.1458	0.17815
$[C_2mim][BF_4]$	198.0	406.11	0.88741	0.19675
$[C_2mim][NTf_2]$	391.3	395.70	1.0479	0.20294
$[C_3mim][NTf_2]$	405.3	349.96	1.0447	0.21223
$[C_4mim][NTf_2]$	419.2	350.76	1.1931	0.15091
$[C_5mim][NTf_2]$	433.4	366.26	1.0835	0.21615
$[C_2mim][EtSO_4]$	236.3	445.45	1.0105	0.17054
$[C_2mim][Triflate]$	260.2	430.75	1.0960	0.13275
$[C_4mim][Triflate]$	288.2	441.12	1.0839	0.16181
$[(C_6H_{13})_3P(C_{14}H_{29})][Cl]$	519.3	384.46	1.4716	0.16515
$[(C_6H_{13})_3P(C_{14}H_{29})][NTf_2]$	374.3	374.30	1.6821	0.13540
$[(C_6H_{13})_3P(C_{14}H_{29})][Ac]$	542.9	401.45	1.5068	0.16242
$[(C_6H_{13})_3P(C_{14}H_{29})][N(CN)_2]$	549.9	375.50	1.5249	0.15537
$[C_4mim][C(CN)_3]$	229.3	425.82	1.1055	0.14946
$[N_{1114}][NTf_2]$	396.4	431.40	1.1769	0.16102
$[C_3mpip][NTf_2]$	422.41	405.45	1.0573	0.23098
$[C_4mpyr][NTf_2]$	422.0	406.35	1.0985	0.13503
$[C_3mpyr][NTf_2]$	408.4	404.92	1.0404	0.23070
$[C_3mpy][NTf_2]$	416.0	411.68	1.0659	0.21706
$[C_6mim][NTf_2]$	447.3	369.04	1.1028	0.21668
$[C_7mim][NTf_2]$	461.0	407.80	1.1294	0.21736
$[C_8mim][NTf_2]$	475.5	398.50	1.1602	0.20981
$[C_{10}mim][NTf_2]$	504.0	403.60	1.4300	0.12271
$[C_4mim][PF_6]$	284.2	379.20	0.96455	0.20574
$[C_6mim][PF_6]$	312.2	398.38	1.05690	0.18236
$[C_8mim][PF_6]$	340.0	404.69	1.08140	0.19568
$[C_4mim][BF_4]$	226.2	390.90	0.97664	0.17889
$[C_6mim][BF_4]$	254.1	396.57	1.03280	0.17872
$[C_8mim][BF_4]$	282.1	445.96	1.0638	0.19783

Fig. 3 displays the linearity of reduced pressure in terms of reduced density for, typically, $[C_4mim][NTf_2]$ and $[(C_6H_{13})_3P(C_{14}H_{29})][N(CN)_2]$ at compressed states and different temperatures. The markers represent the experimental isotherms of Goncalves et al. [37] and Azevedo et al. [38]; solid lines are those calculated by means of the proposed EOS. As the figure illustrates, the regularity of linearity associated with isotherms of $[C_4mim][NTf_2]$ and $[(C_6H_{13})_3P(C_{14}H_{29})][N(CN)_2]$ can be shown well by the present model.

Fig. 4 plots the experimental densities of several studied ILs in

Table 3. Density prediction of ILs studied in this work

Ionic liquid	ΔP (MPa)	ΔT (K)	NP[a]	AAD[b] (%)	Reference
$[C_2mim][NTf_2]$	0.1-30	293-393	096	0.33	[38]
$[C_3mim][NTf_2]$	0.1-60	298-333	165	0.20	[40]
$[C_4mim][NTf_2]$	0.1-60	298-328	168	0.18	[39]
	0.1-35	293-393	080	0.28	[41]
$[C_2mim][EtSO_4]$	0.1-40	293-415	046	1.04	[51]
	0.1-35	298-333	063	0.54	[52]
$[C_2mim][Triflate]$	0.1-35	293-393	091	0.34	[42]
$[(C_6H_{13})_3P(C_{14}H_{29})][Ac]$	0.2-65	298-333	144	0.26	[43]
	0.2-65	298-333	134	0.11	[43]
$[(C_6H_{13})_3P(C_{14}H_{29})][Cl]$	0.1-35	273-318	072	0.18	[37]
$[(C_6H_{13})_3P(C_{14}H_{29})][NTf_2]$	0.2-65	298-333	126	0.11	[43]
$[(C_6H_{13})_3P(C_{14}H_{29})][N(CN_2)]$	0.1-35	273-318	100	0.07	[37]
	0.1-65	293-338	155	0.16	[41]
$[C_6mim][NTf_2]$	0.1-60	293-333	163	0.25	[38]
$[C_8mim][NTf_2]$	0.1-30	293-393	096	0.27	[49]
$[C_4mim][Triflate]$	0.1-10	293-393	077	0.21	[44]
$[C_6mim][BF_4]$	1-200	313-472	180	0.50	[45]
	1-200	313-452	168	0.59	[47]
$[C_4mim][BF_4]$	0.1-60	298-333	068	1.50	[49]
	0.1-20	293-353	020	1.42	[50]
$[C_8mim][BF_4]$	0.1-10	313-452	077	0.23	[44]
$[C_2mim][BF_4]$	1-200	313-472	180	0.63	[45]
$[C_7mim][NTf_2]$	0.1-30	293-333	096	0.25	[42]
$[C_{10}mim][NTf_2]$	0.1-35	298-353	080	0.35	[46]
$[N_{1114}][NTf_2]$	0.1-35	298-353	036	0.28	[25]
$[C_4mim][OcSO_4]$	1-200	313472	178	0.48	[47]
$[C_2mim][OcSO_4]$	0.1	273363	018	0.24	[48]
$[C_4mim][C(CN)_3]$	0.1-30	293-393	096	0.35	[39]
$[C_3mpyr][NTf_2]$	0.1-35	293-393	091	0.29	[40]
$[C_3mpy][NTf_2]$	0.1-35	293-393	091	0.30	[40]
$[C_4mpyr][NTf_2]$	0.1-35	293-393	091	0.35	[40]
$[C_3mpip][NTf_2]$	0.1-35	293-393	091	0.27	[40]
$[C_4mim][PF_6]$	1-200	312.8-432	153	0.52	[47]
$[C_6mim][PF_6]$	1-200	313-372	180	0.46	[45]
$[C_8mim][PF_6]$	1-200	312.8-472	180	0.48	[45]
$[C_5mim][NTf_2]$	0.1-60	298-333	165	0.14	[40]
Overall			3997	0.38	

[a]NP represents the number of data points examined

[b]$AAD = 100/NP \sum_{i=1}^{NP} |\rho_{i,Cal.} - \rho_{i,Exp.}| / \rho_{i,Exp.}$

terms of the calculated ones using the proposed model. Fig. 4 reconfirms the reliability of the proposed model to predict the PVT properties of ILs. The experimental data on density were chosen randomly from the literature [25,40,41,43,47] over the pressure range from 0.1 MPa to 150 MPa and temperature range from 293.15 K to 452 K.

In general, the accuracies of the calculated densities using the proposed EOS were to within ±1.8%.

The modified ISM EOS has been further assessed by comparing with our previous work [17]. Table 4 contains the AAD of the calculated densities of several phosphonium- and imidazolium-based ILs using the present and previous models from the literature values [38,39,41-44,47]. Table 4 clearly demonstrates the superiority of the present work over the previous one [17].

It is a matter of considerable practical importance to compare the present EOS with other empirical methods proposed in the literature. In this respect, we have compared our model with the methods of G &C [24] and Jacquemin et al. (JAC) [25]. The results of the calculations for 17 ILs are gathered in Table 5. In general, our model surpasses the two other methods.

As already stated, in this work, an EOS that was previously constructed for pure substances using statistical-mechanical perturba-

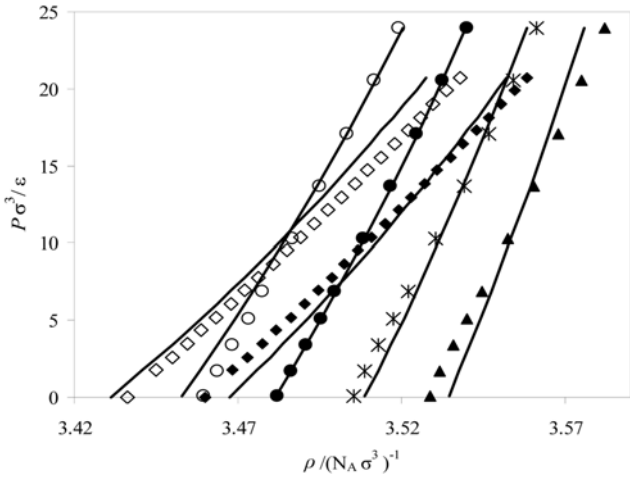

Fig. 3. The reduced pressure vs. reduced density for $[C_4mim][NTf_2]$ and $[(C_6H_{13})_3P(C_{14}H_{29})][N(CN)_2]$. The markers represent the experimental isotherms of Goncalves et al. [37] and Azevedo et al. [38]. Solid lines are those predicted from the proposed EOS for $[C_4mim][NTf_2]$ at 318.14 K (◆), 328.2 K (◇) and $[(C_6H_{13})_3P(C_{14}H_{29})][N(CN)_2]$ at 283.15 K (▲), 293.15 K (∗), 303.15 K (●) and 313.15 K (○).

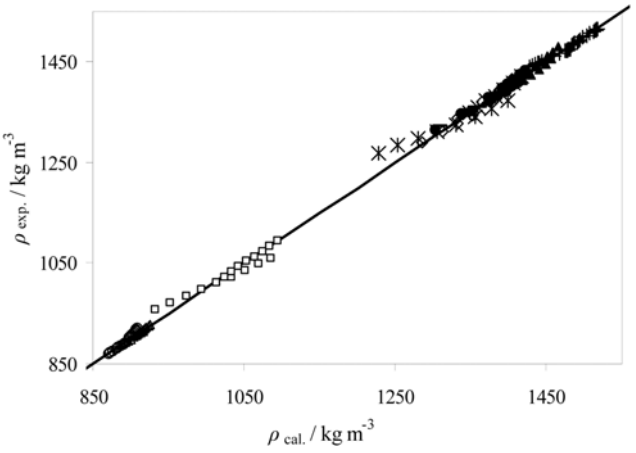

Fig. 4. Shows linear relationship of experimental densities (straight solid line) vs. calculated densities (markers) of ionic liquids at compressed states: $[C_4mim][OcSO_4]$ (□), $[C_4mim][PF_6]$ (∗), $[C_3mim][NTf_2]$ (+), $[C_4mpip][NTf_2]$ (–), $[C_4mpyr][NTf_2]$ (●), $[(C_6H_{13})_3P(C_{14}H_{29})][Cl]$ (○), $[(C_6H_{13})_3P(C_{14}H_{29})][N(CN)_2]$ (△), $[N_{1114}][NTf_2]$ (◇) and $[C_3mpy][NTf_2]$ (▲). The data randomly chosen from the literature [25,40-42,47] over the entire pressure and temperature range from 0.1-200 MPa and 293.15-452 K, respectively.

tion theory, has been extended to mixtures containing ILs. Table 6 reports the AAD of the calculated densities and V^E of studied binary mixtures from the measurements [48,53-57] at various mole fractions and temperatures. Besides, the maximum deviation (MD in %) of the calculations has also been included in Table 6. In the case of binary mixtures, from 898 experimental data points examined, overall AAD of estimated properties using proposed model was found to be 0.43%. The uncertainty associated with the calculated volumetric properties of all binary mixtures studied in this work was found to be ±1.89%. Table 7 compares the present model with the method proposed by G & C [24]. Interestingly, the results are in favor of the superiority of the present model over the G & C model [24]. The AAD of the calculated density and V^E using present model and G & C model for 455 experimental data points [56,57] examined for the selected binary mixtures IL+IL were found to be 0.51% and 0.88%, respectively.

Finally the excess volumetric behavior of binary mixtures IL+water using proposed model has been displayed in Figs. 5 and 6. The positive deviation of the excess molar volumes for $[C_4mim][BF_4]$+water and $[C_2mim][BF_4]$+water over the whole range of compositions and temperatures indicates a repulsive intermolecular potential energy between unlike particles in the mixture. This can be attributed to the high relative permittivity of water, which gives rise to weakening or breaking the strong like electrostatic attractions between the ions, which results in expanding the volume of the binary mix-

Table 4. Comparison of AAD calculated high-pressure densities of studied ILs by the use of model developed in this work and those estimated by the our preceding work [17]

Ionic liquid	ΔT (K)	NP[b]	AAD (%)[a]		
			Previous work [17]	This work	Reference
$[C_2mim][NTf_2]$	293-393	096	0.46	0.33	[39]
$[C_4mim][NTf_2]$	298-333	168	0.62	0.18	[38]
$[C_4mim][OcSO_4]$	313-472	178	1.44	0.48	[47]
$[C_2mim][EtSO_4]$	293-393	080	0.38	0.28	[41]
$[C_2mim]$[Triflate]	293-393	091	0.41	0.34	[42]
$[(C_6H_{13})_3P(C_{14}H_{29})][Cl]$	298-333	134	0.88	0.11	[43]
$[(C_6H_{13})_3P(C_{14}H_{29})][NTf_2]$	298-334	126	0.97	0.11	[43]
$[C_6mim][NTf_2]$	293-338	155	0.89	0.16	[41]
$[C_8mim][BF_4]$	313-393	077	0.17	0.23	[44]
$[C_8mim][NTf_2]$	293-393	096	0.46	0.27	[39]
Overall		1198	0.75	0.24	

[a] $AAD = 100/NP\sum_{i=1}^{NP}|\rho_{i,Cal.} - \rho_{i,Exp.}|/\rho_{i,Exp.}$

[b] NP represents the number of data points examined

Table 5. Shows AAD of calculated densities using proposed EOS with those obtained from the work of JAC [25] and G & C [24], compared with the experiment

Ionic liquid	$T_{min}-T_{max}$ (K)	NP[b]	AAD (%)[a]		G & C [24]	Ref.
			This work	JAC [25]		
$[C_4mim][OcSO_4]$	313-472	174	0.49	0.91	1.41	[47]
$[C_3mim][NTf_2]$	298-333	165	0.20	0.07	0.34	[40]
$[C_4mim][NTf_2]$	298-328	168	0.18	0.23	0.36	[38]
$[C_2mim][EtSO_4]$	298-333	063	0.54	1.08	0.46	[52]
$[C_2mim][Triflate]$	298-333	091	0.34	0.82	0.18	[42]
$[(C_6H_{13})_3P(C_{14}H_{29})][Cl]$	298-333	134	0.11	0.49	0.16	[43]
$[(C_6H_{13})_3P(C_{14}H_{29})][NTf_2]$	298-333	126	0.11	0.16	0.11	[43]
$[(C_6H_{13})_3P(C_{14}H_{29})][Ac]$	298-333	144	0.26	0.06	0.15	[43]
$[C_5mim][NTf_2]$	298-333	165	0.14	0.28	0.27	[40]
$[C_6mim][NTf_2]$	298-333	163	0.26	0.64	0.25	[38]
$[C_8mim][NTf_2]$	293-393	096	0.27	0.39	0.07	[39]
$[C_4mim][Triflate]$	293-393	077	0.21	0.33	0.03	[44]
$[C_8mim][BF_4]$	313-452	077	0.23	0.39	0.03	[44]
$[C_7mim][NTf_2]$	293-393	096	0.25	0.25	0.06	[41]
$[C_4mim][BF_4]$	313-472	189	0.61	1.80	2.42	[47]
$[C_4mpyr][NTf_2]$	298-348	091	0.35	0.56	0.09	[42]
$[C_4mim][PF_6]$	313-472	189	0.72	1.49	2.17	[47]
Overall		2112	0.32	0.62	0.65	

[a] $AAD = 100/NP\sum_{i=1}^{NP}|\rho_{i,Cal.}-\rho_{i,Exp.}|/\rho_{i,Exp.}$

[b] NP represents the number of data points examined

Table 6. Average absolute deviation (AAD) of predicted densities and V^E of binary mixtures containing IL+IL and IL+water using proposed EOS, compared with the experiment

Mixture	ΔT(K)	NP[a]	AAD (%)	MD (%)[d]	Ref.
$[C_2mim][BF_4]$+water	293-323	076	0.37[b]	−0.93	[53]
$[C_4mim][BF_4]$+water	303-353	076	0.32[b]	−1.09	[48]
$[C_4mim][Triflate]$+water	278-338	076	0.46[b]	−0.98	[54]
$[C_4mim][C(CN)_3]$+water	278-358	080	0.36[b]	−0.91	[55]
$[C_2mim][BF_4]$+$[C_6mim][BF_4]$	298-308	134	0.59[b]	−1.12	[56]
$[C_4mim][BF_4]$+$[C_6mim][BF_4]$	298-308	108	0.58[b]	−0.88	[56]
$[C_4mim][BF_4]$+$[C_4mim][PF_6]$	298-308	125	0.60[b]	−1.05	[56]
$[C_4mim][BF_4]$+$[C_4mim][PF_6]$	298-333	010	0.29[c]	−0.65	[57]
$[C_2mim][NTf_2]$+$[C_{10}mim][NTf_2]$	298-333	014	0.27[c]	−0.66	[57]
$[C_4mim][NTf_2]$+$[C_{10}mim][NTf_2]$	298-333	008	0.25[c]	−0.62	[57]
$[C_6mim][NTf_2]$+$[C_{10}mim][NTf_2]$	298-333	014	0.26[c]	−0.54	[57]
$[C_8mim][NTf_2]$+$[C_{10}mim][NTf_2]$	298-333	006	0.21[c]	−0.56	[57]
$[C_4mim][NTf_2]$+$[C_8mim][NTf_2]$	298-333	008	0.26[c]	−0.47	[57]
$[C_2mim][NTf_2]$+$[C_8mim][NTf_2]$	298-333	010	0.29[c]	−0.49	[57]
$[C_4mim][BF_4]$+$[C_4mim][NTf_2]$	298-333	016	0.33[c]	−0.81	[57]
$[C_2mim][BF_4]$+water	293-323	067	0.35[c]	−0.63	[53]
$[C_4mim][BF_4]$+water	303-353	071	0.34[c]	−0.66	[48]
Overall		898	0.43		

[a] NP represents the number of data points examined

[b] $AAD = 100/NP\sum_{i=1}^{NP}|\rho_{i,Cal.}-\rho_{i,Exp.}|/\rho_{i,Exp.}$

[c] $AAD = 100/NP\sum_{i=1}^{NP}|V^E_{i,Cal.}-V^E_{i,Exp.}|/V^E_{i,Exp.}$

[d] MD represents the maximum deviation of calculated $\rho_{mix.}$ and V^E

Table 7. Comparison of the AAD of calculated density and V^E of binary mixtures in this work and those obtained by the method of G & C [24], compared with the literature data

Mixture	NP[a]	This work	G & C [24]	Ref.
$[C_2mim][BF_4]+[C_6mim][BF_4]$	134	0.59[b]	1.24	[56]
$C_4mim][BF_4]+[C_6mim][BF_4]$	108	0.58[b]	0.60	[56]
	126	0.60[b]	0.14	[56]
$[C_4mim][BF_4]+[C_4mim][PF_6]$	010	0.29[c]	0.13	[57]
$[C_2mim][NTf_2]+[C_{10}mim][NTf_2]$	014	0.27[c]	2.63	[57]
$[C_4mim][NTf_2]+[C_{10}mim][NTf_2]$	008	0.25[c]	2.09	[57]
$[C_6mim][NTf_2]+[C_{10}mim][NTf_2]$	014	0.26[c]	1.62	[57]
$[C_8mim][NTf_2]+[C_{10}mim][NTf_2]$	006	0.21[c]	2.08	[57]
$[C_4mim][NTf_2]+[C_8mim][NTf_2]$	008	0.26[c]	0.64	[57]
$[C_2mim][NTf_2]+[C_8mim][NTf_2]$	010	0.29[c]	1.01	[57]
$[C_4mim][BF_4]+[C_4mim][NTf_2]$	016	0.33[c]	0.79	[57]
Overall	455	0.51	0.88	

[a]NP represents the number of data points examined

[b] $AAD=100/NP\sum_{i=1}^{NP}|\rho_{i,Cal.}-\rho_{i,Exp.}|/\rho_{i,Exp.}$

[c] $AAD=100/NP\sum_{i=1}^{NP}|V^E_{i,Cal.}-V^E_{i,Exp.}|/V^E_{i,Exp.}$

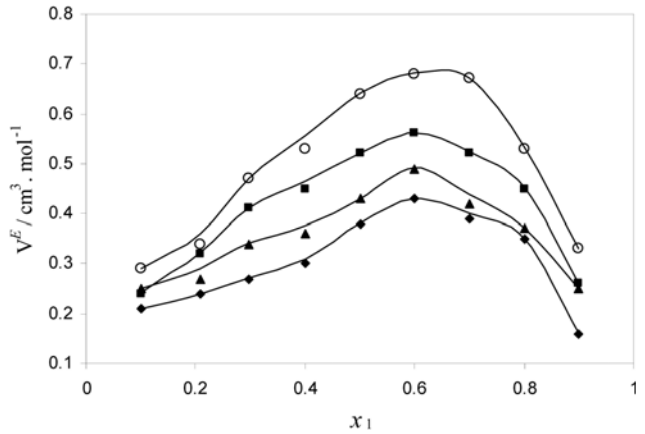

Fig. 5. Excess molar volume of mixture $[C_4mim][BF_4]$ (x_2)+water (x_1) as a function of mole fraction (x) of water at temperatures: 303 K (◆), 313.15 K (▲), 323.15 K (■) and 333.15 K (○). The solid line represents the calculated V^E from proposed EOS and the corresponding markers are the experiment values [48].

ture from the pure IL. The increase of the V^E with temperature indicates that the mixture is more expansible than the pure compounds. Thus the temperature increase gives rise to loosening aggregation in pure IL.

CONCLUSION

We have successfully applied the ISM equation of state to ILs and their mixtures using new corresponding states correlations for second virial coefficients, α(T) and b(T). On the basis of the results tabulated herein, the following conclusions can be drawn: 1) when tested against experimental data, the calculated liquid densities gave

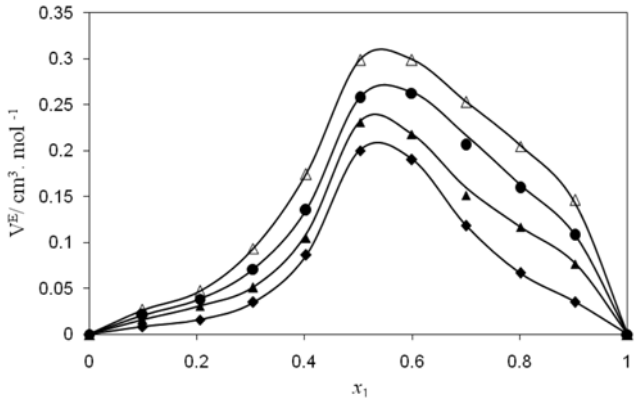

Fig. 6. Excess molar volume of mixture $[C_2mim][BF_4]$ (x_2)+water (x_1) as a function of mole fraction (x) of water at temperatures: 293.15 K (◆), 303.15 K (▲), 313.15 K (●) and 323.15 K (unfilled triangle). The solid line represents the calculated V^E from proposed EOS and the corresponding markers are the experiment values [53].

the mean average absolute deviations of 0.38%. 2) When compared with our previous work, we showed that the accuracy of the ISM EOS can be further improved using two adjustable scaling parameters ε and σ. 3) To assess the modified ISM EOS further, we compared it with other empirical methods such as G & C and Jacquemin et al. (JAC) reported in literature. In general, the present model outperforms the two other methods.

Finally, the proposed EOS has been successfully extended to predict volumetric properties of several binary mixtures including IL+IL and of IL+water over a wide range of temperatures and compositions.

This study demonstrates that once the second virial coefficient from the microscopic corresponding-states correlation equation, the values of λ from some high-density information, and the two constants ε and σ for each ILs in conjunction with a simple combining rule for estimating the cross values of these parameters are known, the entire EOS can be employed to predict the volumetric behaviors of fluid mixtures.

ACKNOWLEDGEMENT

We are grateful to the research committee of Shiraz University and Shiraz University of Technology for supporting this project.

NOMENCLATURE AND UNITS

b(T) : van der Waals covolume [m^3]
P : pressure [Pa]
R : gas constant [J/mole·K]
T : absolute temperature [K]
k_B : Boltzmann constant [J/K]
B_2(T) : second virial coefficient [m^3]
a_1-c_2 : the coefficients that used in Eqs. (7)-(8)
G : average pair distribution function of non-spherical hard-convex bodies at contact
V^E : excess molar volume
u(r) : pair potential function

Greek Letters

ε : non-bonded interaction energy parameter [J]
σ : effective hard-sphere diameter [nm]
ξ_3 : parameter in Eq. (12)
α(T) : contribution of repulsive branch of pair potential function [J/m^3]
λ : free parameter
ρ : molar density [mol/m^3]

Subscripts

r : reduced

Superscripts

vap : vaporization

REFERENCES

1. B. Garcia, S. Lavallee, G. Perron, C. Michot and M. Armand, *Electrochim. Acta*, **49**, 4583 (2004).
2. T. Sato, G. Masuda and K. Takagi, *Electrochim. Acta*, **49**, 3603 (2004).
3. M. J. Earle and K. R. Seddon, *Pure. Appl. Chem*., **72**, 1391 (2000).
4. B. Wu, R. G. Reddy and R. D. Rogers, *Proceedings of Solar Forum*, 2001, Solar Energy: The Power to Choose, April 21-25, ASME, Washington, DC (2001).
5. J. Wang, Z. Li, C. Li and Z. Wang, *Ind. Eng. Chem. Res*., **49**, 4420 (2010).
6. C. Shen, C. Li, X. Li, Y. Lu and Y. Muhammad, *Chem. Eng. Sci*., **66**, 2690 (2011).
7. H. Machida, Y. Sato and R. L. Smith Jr., *Fluid Phase Equilib*., **297**, 205 (2010).
8. J. Abildskov, M. D. Ellegaard and J. P. O'Connell, *Fluid Phase Equilib*., **286**, 95 (2009).
9. J. Abildskov, M. D. Ellegaard and J. P. O'Connell, *Fluid Phase Equilib*., **295**, 215 (2010).
10. J. Abildskov, M. D. Ellegaard and J. P. O'Connell, *J. Supercrit. Fluid*, **55**, 833 (2010).
11. J. Palomar, V. R. Ferro, J. S. Torrecilla and F. Rodriguez, *Ind. Eng. Chem. Res*., **46**, 6041 (2007).
12. S. Trohalaki, R. Pachter, G. Drake and T. Hawkins, *Energy Fuels*, **19**, 279 (2005).
13. J. O. Valderama, A. Reategui and R. E. Rojas, *Ind. Eng. Chem. Res*., **48**, 3254 (2009).
14. S. Aparicio, M. Atilhan and F. Karadas, *Ind. Eng. Chem. Res*., **49**, 9580 (2010).
15. Y. S. Kim, W. Y. Choi, J. H. Jang, K.-P. Yoo and C. S. Lee, *Fluid Phase Equilib*., **228-229**, 439 (2005).
16. Y. Song and E. A. Mason, *J. Chem. Phys*., **91**, 7840 (1989).
17. S. M. Hosseini and Z. Sharafi, *Ionics*, **17**, 511 (2011).
18. S. M. Hosseini, J. Moghadasi, M. M. Papari and F. Fadaie-Nobandegani, *Ind. Eng. Chem. Res.*, **51**, 758 (2012).
19. S. M. Hosseini, *Ionics*, **16**, 571 (2010).
20. S. M. Hosseini, J. Moghadasi and M. M. Papari, *Ionics*, **16**, 757 (2010).
21. S. M. Hosseini, J. Moghadasi, M. M. Papari and F. Fadaie-Nobandegani, *J. Mol. Liq*., **160**, 67 (2011).
22. J. O. Valderrama and P. A. Robles, *Ind. Eng. Chem. Res*., **46**, 1338 (2007).
23. J. O. Valderrama and R. E. Rojas, *Ind. Eng. Chem. Res*., **48**, 6890 (2009).
24. R. L. Gardas and J. A. P. Coutinho, *Fluid Phase Equilib*., **263**, 26 (2008).
25. J. Jacquemin, P. Nancarrow, D. W. Rooney, M. F. Costa Gomes, P. Husson, V. Majer, A. A. H. Padua and C. Hardacre, *J. Chem. Eng. Data*, **53**, 2133 (2008).
26. J. Jacquemin, G. Rile, P. Nancarrow, D. W. Rooney, M. F. Costa Gomes, A. A. H. Padua and C. Hardacre, *J. Chem. Eng. Data*, **53**, 716 (2008).
27. C. Ye and J. M. Shreeve, *J. Phys. Chem. A*, **111**, 1456 (2007).
28. F. M. Tao and E. A. Mason, *Int. J. Thermophys*., **13**, 1053 (1992).
29. A. Boushehri and E. A. Mason, *Int. J. Thermophys*., **14**, 685 (1993).
30. M. H. Ghatee and A. Boushehri, *Int. J. Thermophys*., **17**, 945 (1996).
31. N. Mehdipour and A. Boushehri, *Int. J. Thermophys*., **19**, 331 (1998).
32. H. Eslami, *Int. J. Thermophys*., **21**, 1123 (2000).
33. S. Sheikh, M. M. Papari and A. Boushehri, *Ind. Eng. Chem. Res*., **41**, 3274 (2002).
34. M. M. Papari, A. Razavizadeh, F. Mokhberi and A. Boushehri, *Ind. Eng. Chem. Res*., **4**, 3802 (2003).
35. Y. Song, *J. Chem. Phys*., **92**, 2683 (1990).
36. S. P. Verevkin, *Angew. Chem. Int. Ed*.,**47**, 5071 (2008).
37. F. A. M. M. Goncalves, C. S. M. F. Costa, C. E. Ferreira, J. C. S. Bernardo, I. Johnson, I. M. A. Fonseca and A. G. M. Ferreira, *J. Chem. Thermodyn*., **43**, 914 (2011).
38. R. Gomes de Azevedo, J. M. S. S. Esperanca, J. Szydlowski, Z. P. Visak, P. F. Pires, H. J. R. Guedes and L. P. N. Rebelo, *J. Chem. Thermodyn*., **37**, 888 (2005).
39. R. L. Gardas, M. G. Freire, P. J. Carvalho, I. M. Marrucho, I. M. A. Fonseca, A. G. M. Ferreira and J. A. P. Coutinho, *J. Chem. Eng. Data*, **52**, 1881 (2007).
40. J. M. S. S. Esperanca, Z. P. Visak, N. V. Plechkova, K. R. Seddon, H. J. R. Guedes and L. P. N. Rebelo, *J. Chem. Eng. Data*, **51**, 2009 (2006).
41. J. M. S. S. Esperança, H. J. R. Guedes, J. N. C. Lopes and L. P. N. Rebelo, *J. Chem. Eng. Data*, **53**, 867 (2008).
42. R. L. Gardas, H. F. Costa, M. G. Freire, P. J. Carvalho, I. M. Marrucho, I. M. A. Fonseca, A. G. M. Ferreira and J. A. P. Coutinho, *J. Chem. Eng. Data*, **53**, 805 (2008).
43. J. M. S. S. Esperanca, H. J. R. Guedes, M. Blesic and L. P. N. Rebelo, *J. Chem. Eng. Data*, **51**, 237 (2006).
44. R. L. Gardas, M. G. Freire, P. J. Carvalho, I. M. Marrucho, I. M. A. Fonseca, A. G. M. Ferreira and J. A. P. Coutinho, *J. Chem. Eng. Data*, **52**, 80 (2007).
45. R. Taguchi, H. Machida, Y. Sato and R. L. Smith Jr., *J. Chem. Eng. Data*, **54**, 22 (2009).
46. L. I. N. Tome, P. J. Carvalho, M. G. Freire, I. M. Marrucho, I. M. A. Fonseca, A. G. M. Ferreira, J. A. P. Coutinho and R. L. Gardas, *J. Chem. Eng. Data*, **53**, 1914 (2008).
47. H. Machida, Y. Sato and R. L. Smith Jr., *Fluid Phase Equilib*., **264**, 147 (2008).
48. Q. Zhou, L. S. Wang and H. P. Chen, *J. Chem. Eng. Data*, 51, 905 (2006).
49. R. G. Azevedo, J. M. S. S. Esperanca,V. Najdanovic-Visak, Z. P. Visak, H. J. R. Guedes, M. N. Ponte and L. P. N. Rebelo, *J. Chem. Eng. Data*, **50**, 997 (2005).

50. D. Tomida, A. Kumagai, K. Qiao and C. Yokoyama, *Int. J. Thermophys.*, **27**, 39 (2006).
51. J. Jacquemin, P. Husson, V. Mayer and I. Cibulka, *J. Chem. Eng. Data*, **52**, 2204 (2007).
52. T. Hofman, A. Go*l*don, A. Nevines and T. M. Letcher, *J. Chem. Thermodyn.*, **40**, 580 (2008).
53. S. Zhang, X. Li, H. Chen, J. Wang, J. Zhang and M. Zhang, *J. Chem. Eng. Data*, **49**, 760 (2004).
54. M. L. Ge, R. S. Zhao,Y. F. Yi, Q. Zhang and L. S. Wang, *J. Chem. Eng. Data*, **53**, 2408 (2008).
55. P. J. Carvalho, T. Regueira, L. M. N. B. F. Santos, J. Fernandez and J. A. P. Coutinho, *J. Chem. Eng. Data*, **55**, 645 (2010).
56. P. Navia, J. Troncoso and L. Romani, *J. Chem. Eng. Data*, **52**, 1369 (2007).
57. J. N. C. Lopes, T. C. Cordeiro, J. M. S. S. Esperanca, H. J. R. Guedes, S. Huq, L. P. N. Rebelo and K. R. Seddon, *J. Phys. Chem. B*, **10**, 3519 (2005).